



Showcasing research from Professor Nishikawa and Ouchi's laboratory, School of Engineering, Kyoto University, Kyoto, Japan.

Property modulation of poly(vinyl alcohol)s *via* controlled incorporation of  $\alpha$ -methyl groups using alkenylboron monomers

Radical copolymerization of vinyl- and isopropenyl-type boron monomers followed by side-chain replacement afforded  $\alpha$ -methylated poly(vinyl alcohol)s inaccessible by conventional methods. Copolymer compositions were widely tunable, yielding amorphous copolymers that exhibited solvent-dependent thermally-responsive behaviors.

Image reproduced by permission of Tsuyoshi Nishikawa from *Polym. Chem.*, 2026, **17**, 903.

As featured in:



See Hiroshi Suzuki, Tsuyoshi Nishikawa and Makoto Ouchi, *Polym. Chem.*, 2026, **17**, 903.

Cite this: *Polym. Chem.*, 2026, **17**, 903

# Property modulation of poly(vinyl alcohol)s via controlled incorporation of $\alpha$ -methyl groups using alkenylboron monomers

Hiroshi Suzuki, Tsuyoshi Nishikawa \* and Makoto Ouchi \*

Radical copolymerization of vinyl- and isopropenyl-type boron monomers followed by side-chain oxidation enabled the synthesis of  $\alpha$ -methylated poly(vinyl alcohol)s (PVAs), which are difficult to obtain by conventional methods. The composition ratio of the resulting vinyl alcohol (VA)–isopropenyl alcohol (IPA) copolymers was tunable in a wide range (VA/IPA = 84/16–7/93 mol%) by adjusting the monomer feed ratio in the copolymerization step. All copolymers were amorphous in the bulk state regardless of their composition ratios, despite the semi-crystalline nature of both VA and IPA homopolymers. In solution, copolymers with specific compositions exhibited solvent-dependent thermal-responsive behavior: lower critical solution temperature (LCST)-type transitions in water and upper critical solution temperature (UCST)-type transitions in acetone.

Received 9th December 2025,  
Accepted 29th January 2026

DOI: 10.1039/d5py01168j

rsc.li/polymers

## Introduction

Poly(vinyl alcohol) (PVA) is an important water-soluble and semi-crystalline polymer that is widely used in adhesives,<sup>1,2</sup> fibers,<sup>3</sup> and polarizing films.<sup>4</sup> The polymer is typically prepared by radical polymerization of vinyl acetate (VAc) followed by saponification (Fig. 1A). The properties of PVA, such as hydrophilicity, crystallinity, and thermal stability, have been tailored through various chemical modifications, most commonly by partial derivatization of the hydroxy groups. Among these, the intramolecular acetal formation of PVA with formaldehyde, pioneered by Sakurada to enhance mechanical strength, represents the most classical example; the resulting polymer, known as vinylon, is industrially used as a high-strength fiber material.<sup>5–7</sup> Partial acetylation has also been employed to fine-tune physical characteristics for specific applications.<sup>8,9</sup> In addition, copolymerization of VAc with other monomers provides a versatile route to modulate PVA properties: ethylene–vinyl alcohol (VA) copolymers are widely used as gas-barrier materials,<sup>10–12</sup> while VA–acrylamide copolymers exhibit reduced crystallinity while retaining hydrophilicity.<sup>13</sup>

Poly(isopropenyl alcohol) (PIPA) is a structural analogue of PVA in which a methyl group is introduced at the  $\alpha$ -position of each repeating unit. The presence of this hydrophobic substi-

tuent of the isopropenyl alcohol (IPA) unit is expected to influence the physical properties of PVA, particularly decreased crystallinity and hydrophilicity. Consequently, PIPA and its copolymers with PVA are of particular interest as chemically modified PVA derivatives with tunable structural and functional characteristics (Fig. 1B). Isopropenyl acetate (IPAc) can be expected as the precursor monomer for constructing the PIPA repeating unit; however, the polymerization is challenging due to its inherently poor (co)polymerization ability. The limitation arises from frequent degenerative chain transfer to the  $\alpha$ -methyl group of the monomer giving less-reactive allyl radical species.<sup>14–16</sup> To minimize the influence of the degenerative chain transfer process, Nishino and coworkers performed the radical polymerization of IPAc under high-pressure conditions (*e.g.*, 1 GPa), successfully obtaining the corresponding polymer.<sup>17</sup> However, such high-pressure conditions require specialized equipment and involve potential safety risks, making this approach less desirable for general use. In previous reports about radical copolymerization of IPAc with VAc under ambient pressure, the increase of IPAc content caused both a significant decrease of the molecular weight of copolymers and an increase in structural errors such as 1,2-glycol bonds.<sup>18,19</sup> Even if the copolymerization proceeds under high-pressure conditions, systematic control of the composition ratio would be difficult to achieve.

In 2019, our group reported the radical polymerization of isopropenylboronic acid pinacol ester (IPBpin) and post-polymerization oxidation to synthesize PIPA.<sup>20–23</sup> We have also investigated radical polymerization of vinylboron compounds and found that their polymerization behavior strongly

Department of Polymer Chemistry, Graduate School of Engineering, Kyoto University, Nishikyo-ku, Kyoto 615-8510, Japan. E-mail: nishikawa.tsuyoshi.8n@kyoto-u.ac.jp, ouchi.makoto.2v@kyoto-u.ac.jp





**Fig. 1** (A) Chemical modifications of PVA via post-polymerization functionalization of PVA or copolymerization of VAc with other comonomers. (B) Difficulty in synthesizing vinyl alcohol (VA)–isopropenyl alcohol (IPA) copolymers using acetate monomers. (C) Synthetic route to VA–IPA copolymers through radical copolymerization of vinylboron and isopropenylboron monomers followed by post-polymerization oxidation enabling composition control (this work).

depends on the protecting group on boron. Pinacol-protected one (VBpin) underwent frequent backbiting during homopolymerization, affording a branched polymer that could be converted into branched PVA via post-polymerization oxidation.<sup>24</sup> In contrast, the use of an anthranilamide-type protecting group bearing a substituent on the amide moiety effectively suppressed backbiting, enabling the synthesis of linear PVA.<sup>25</sup> These findings led us to envision that the copolymerization of isopropenylboron and vinylboron monomers, followed by post-polymerization oxidation would provide a series of PVAs bearing the  $\alpha$ -methyl group in tunable ratios (Fig. 1C). Consequently, we achieved syntheses of VA–IPA copolymers in some ratios and examined impacts of the  $\alpha$ -methyl groups on

crystallinity in bulk and solubility/thermoresponsivity in common solvents such as water.

## Results and discussion

We performed radical copolymerization of IPBpin as the isopropenyl-type boron monomer with a vinyl-type boron monomer and compared their copolymerization behavior with that of acetyl-type monomers (VAc and IPAc) (Fig. 2A and S1). As the vinyl-type boron monomer, we selected an anthranilamide-protected vinylboron monomer bearing a 2-methoxyethyl substituent on the  $N_{amide}$  (VBaam-MOE). In our previous





**Fig. 2** (A) Time–conversion plots and molar mass of the resulting polymers in radical copolymerization of vinyl monomers (VBaam-MOE or VAc) with isopropenyl monomers (IPBpin or IPAc) in DMF at 30 °C:  $[\text{vinyl monomer}]_0 = [\text{isopropenyl monomer}]_0 = 750 \text{ mM}$  and  $[\text{V-70}]_0 = 15 \text{ mM}$ . (B) Correlation between  $M_n$  of the resulting copolymer and the feed ratio of the vinyl monomer in the radical copolymerization of IPBpin with VBaam-MOE (solid circles) or VBpin (open circles). (C) Copolymer–composition curve for copolymerization of VBaam-MOE ( $M_1$ ) and IPBpin ( $M_2$ ).

study, we elucidated the key characteristics of VBaam-MOE as a monomer for radical polymerization: (i) backbiting chain transfer is effectively suppressed due to the steric effect of the  $N_{\text{amide}}$  substituent; (ii) both of the monomer and the resulting polymer exhibit high solubility in organic solvents thanks to the methoxyethyl group; and (iii) the polymerization proceeds at a higher rate than other anthranilamide-protected boron monomers.<sup>25</sup> The polymerization conditions were as follows:  $[\text{VBaam-MOE}]_0/[\text{IPBpin}]_0/[\text{V-70}]_0 = 750/750/15 \text{ mM}$  in DMF at 30 °C. The copolymerization smoothly proceeded giving high conversion, and their consumption speed was almost the same as each other [conv.(VBaam-MOE) = 85%, conv.(IPBpin) = 89%, 48 h]. The number-average molecular weight ( $M_n$ ) of the resultant copolymer was 16 000. On the other hand, when radical copolymerization of two acetyl monomers (VAc and IPAc) was performed under the same conditions, they were hardly consumed [conv.(VAc) = 13%, conv.(IPAc) = 8%, 48 h] and the product was an oligomer ( $M_n = 2400$ ). In the copolymerization under bulk conditions, the  $M_n$  increased to 7600, but the monomer conversion was still low [conv.(VAc) = 28%, conv.(IPAc) = 15%, 48 h] (Fig. S2). The combinations of boron- and acetyl-monomers, such as VBaam-MOE/IPAc, IPBpin/VAc, were also tested. In these cases, the boron monomers were consumed faster than the acetyl monomers and the conversion

of the latter was very low: conv.(VBaam-MOE) = 87% vs. conv.(IPAc) = 18%, conv.(IPBpin) = 46% vs. conv.(VAc) = 5% in 48 h. The boron-containing monomers behave as conjugated monomers, whereas the acetyl monomers are non-conjugated, and there is no significant difference in the electron density between the two types of monomers: therefore, the poor copolymerizability of their combination is a reasonable outcome.

The excellent copolymerizability of the VBaam-MOE/IPBpin combination is likely attributed to the fact that VBaam-MOE does not undergo backbiting chain-transfer reactions. To verify this assumption, we examined the copolymerization of VBpin, which is known to promote the backbiting chain-transfer reaction in the homopolymerization, instead of VBaam-MOE. As expected, the molecular weight of the resultant copolymer ( $M_n = 9500$ , Fig. S3) was significantly lower despite the comparable conversion to the pair of VBaam-MOE and IPBpin [conv.(VBpin) = 69%, conv.(IPBpin) = 64%, 48 h]. Effects of injection ratio on the molecular weight of the resultant copolymer were also examined. In the case of VBpin, the  $M_n$  value decreased as the VBpin content in the feed increased, and the  $M_n$  became less than 5000 when the injection ratio of VBpin was 80 mol% (Fig. 2B and Table S1). The conversions of both monomers also decreased with increasing VBpin injection, becoming below 50% when 80 mol% of VBpin was used. In contrast,



when VBaam-MOE was used, an entirely different trend was observed: the  $M_n$  value rather increased as the monomer feed increased maintaining high conversions (>90%). The distinct copolymerization behavior clearly reflects the ability of VBaam-MOE to suppress chain-transfer reactions unlike VBpin, confirming the superior copolymerizability of VBaam-MOE with IPBpin. Furthermore, the monomer reactivity ratios for the copolymerization of VBaam-MOE and IPBpin were determined ( $M_1$  = VBaam-MOE,  $M_2$  = IPBpin, Fig. 2C and Table S2). Both  $r_1$  and  $r_2$  were lower than 1 ( $r_1 = 0.302$ ,  $r_2 = 0.567$ ), indicating that the cross-over propagation between different monomers is rather preferred over the consecutive propagation of the same monomers.

2-Cyano-2-propyl dodecyl trithiocarbonate (CPDT) was available as a chain transfer agent (CTA) for control of radical copolymerization of VBaam-MOE and IPBpin *via* the reversible addition-fragmentation chain transfer (RAFT) process. Regardless of the injection ratio, the molecular weights of the resultant copolymers increased linearly with monomer conversion and the molecular weight distributions ( $D_s$ ) were narrow

[ $D < 1.5$ , Fig. S4–S7 for  $[VBaam-MOE]_0/[IPBpin]_0 = 2/1, 1/1, 1/2$  (molar ratio) actual concentrations are given in the SI].

Post-polymerization oxidation was performed for the copolymers and homopolymers. A series of copolymers and homopolymers was prepared through free radical (co)polymerization of VBaam-MOE and/or IPBpin with different monomer injection ratios  $[[VBaam-MOE]_0/[IPBpin]_0 = 10/1, 4/1, 2/1, 1/1, 1/2, 1/4, \text{ and } 1/10$  (molar ratio) for copolymerization, actual concentrations are shown in the SI]. The  $^1H$  NMR spectra of the resultant copolymers indicated that the IPBpin unit composition ratio could be tuned from 10 mol% to 90 mol% (Fig. S8–S16 and Table S3). We attempted the oxidation of the copolymer with  $H_2O_2$  and NaOH to convert into VA-IPA copolymers and purification of the product by dialysis. The  $^1H$  NMR spectrum of the product indicated the quantitative transformation, but unidentified peaks from aromatic protons were also detected. The peaks likely arise from the byproducts generated by oxidation of the anthranilamide pendant and the removal from the copolymers was found to be difficult.<sup>26</sup> The difficulty in removal of these byproducts by dialysis may be ascribed to the



Fig. 3 Transformation of VBaam-MOE-IPBpin (co)polymers to VA-IPA (co)polymers through protecting group (PG) replacement from anthranilamide to pinacol and subsequent oxidation. (A)  $^1H$  NMR and (B) FT-IR spectra of the resulting VA-IPA (co)polymers.



relatively large molecular size and low polarity, making the diffusion in the dialysis membrane slow. We then decided to replace the anthranilamide protection with pinacol using *p*-toluenesulfonic acid (TsOH), followed by the oxidation reaction (Fig. S17–S25). The two steps transformation was effective for the copolymers containing more than 20 mol% VBaam-MOE units. Consequently, VA–IPA copolymers of various composition ratios were successfully obtained as supported by structural analyses by  $^1\text{H}$  NMR (Fig. 3A, DMSO- $d_6$ ): the peaks from the boron protecting group (*i.e.*, pinacol and anthranilamide) completely disappeared, and the peak from the byproduct was hardly observed. Most importantly, the signals from the hydroxy group ( $c_1$  for PVA and  $c_2$  for PIPA) were clearly detected at 4.2–4.7 ppm for  $c_1$  and at 5.1–5.5 ppm for  $c_2$  protons. The three sharp peaks arising from the hydroxy group in PVA ( $c_1$ ) are known to correspond to triad tacticity (*mm*, *mr*, *rr*). Although detailed studies have not yet been reported, the hydroxy-derived signals of PIPA ( $c_2$ ) also split into distinct sharp peaks, which are likely due to tacticity. A particularly noteworthy finding was that the NMR spectra of the respective homopolymers (PVA and PIPA) exhibited hydroxy-derived signals at distinct chemical shifts, while for the copolymers, the hydroxyl peaks shifted to the intermediate position between those of PVA and PIPA ( $\sim 4.9$  ppm) progressively with composition. Together with the monomer reactivity ratios, these results suggest that the two repeating units are incorporated in a random fashion with a slight preference for an alternating sequence along the polymer chain. When one repeating unit component (VA or IPA) predominated in the copolymer composition, distinct splitting of the hydroxy peaks due to stereoregularity was observed. This is probably due to that con-

tinuous sequences of identical units are present. However, as the compositional difference between the two monomers decreased, the proportion of such continuous sequences became smaller, and the hydroxy-derived signals appeared broadened instead. The composition ratio was determined by peak integrations of methine protons in the VA unit ( $b_1$ ) and methylene/methyl protons in both units ( $a_1$ ,  $a_2$ , and  $b_2$ ); VA/IPA = 84/16, 73/27, 57/43, 45/55, 31/69, 18/82 and 7/93 mol%. These values were almost consistent with the composition ratios (VBaam-MOE/IPBpin) before transformation. In contrast to the drastic changes observed in the hydroxy-derived peaks in the  $^1\text{H}$  NMR spectra depending on the VA/IPA composition, the FT-IR absorption band corresponding to the hydroxy groups at around  $3300\text{ cm}^{-1}$  showed almost no noticeable change (Fig. 3B).

We then performed differential scanning calorimetry (DSC) and X-ray diffraction (XRD) of the thus-obtained VA–IPA (co) polymers to investigate impact of the  $\alpha$ -methyl group on the crystallization behavior (Fig. 4 and S26–S35). As for the PVA homopolymer obtained from VBaam-MOE, the exothermic peak derived from melting of the crystallized polymer was detected at  $198\text{ }^\circ\text{C}$ . In the XRD profile, the characteristic peaks corresponding to the diffractions of the lattice surfaces of PVA crystalline [(100), (10 $\bar{1}$  and 101), (200), and (11 $\bar{1}$  and 111)]<sup>27</sup> were observed. PIPA also showed an endothermic melting peak at  $127\text{ }^\circ\text{C}$ , indicating the semi-crystalline nature of PIPA. Two sharp peaks in the XRD profile also supported the crystallization.<sup>28</sup> On the other hand, PIPA prepared by high-pressure polymerization of IPAc has been previously reported as an amorphous polymer.<sup>17</sup> This difference is probably due to the structural defects such as the branch structure and head-to-



Fig. 4 Physical properties of VA–IPA (co)polymers: (A) DSC curves (second heating at  $10\text{ }^\circ\text{C min}^{-1}$ ) and (B) XRD profiles.



head generated under harsh polymerization conditions. Tacticity is also an important factor that may contribute to the distinct crystallization behavior depending on the precursor monomer. However, the investigation on the correlation between tacticity and crystallinity is highly challenging at this stage.

Whereas both homopolymers exhibited crystallinity, all copolymers synthesized in this study were amorphous. Notably, only the copolymer with a composition ratio of VA/IPA = 84/16 showed a small endothermic peak at 148 °C in the DSC trace, which may correspond to melting of crystalline domains; however, the peak was too weak for the polymer to be regarded as crystalline. Instead, baseline shifts from the glass transition were observed in the DSC trace and the glass transition temperature ( $T_g$ ) gradually decreased with the increase of IPA content. Intriguingly, the copolymer with a composition ratio of 45/55 specifically exhibited a relatively high  $T_g$ . Both reactivity ratios are lower than 1 ( $r_1 = 0.302$ ,  $r_2 = 0.567$  for  $M_1 = \text{VBaam-MOE}$ ,  $M_2 = \text{IPBpin}$ ), thus the copolymerization at 1 : 1 feed ratio is expected to yield a copolymer with a moderately alternating tendency and a limited amount of homosequences. Therefore, the enhanced  $T_g$  may result from the heterosequence-rich structure, but this speculation will require more precise control of the copolymers. XRD profiles also supported the amorphous character of VA-IPA copolymers; most of the copolymers did not display sharp diffraction peaks in the XRD patterns. Exceptionally, the VA-rich copolymer (VA/IPA = 84/16) gave very tiny XRD peaks, suggesting the slight crystallinity corresponding to the small endothermic peak in the DSC traces of the same copolymer. The face distances ( $d$ ) calculated from the most intense peaks increased (4.57 Å → 6.11 Å) as the IPA unit ratio (0 mol% → 100 mol%) probably because the introduced methyl groups increased the occupied volume of polymers (Table S4).

Finally, we investigated the solubility of VA-IPA (co)polymers in various common solvents including water as well as the thermo-responsive behavior of the solution. They showed different solubilities depending on the copolymerization ratio (Fig. 5A and S36). PVA was soluble in water, whereas PIPA was insoluble: the hydrophobic methyl group causes a decrease in hydrophilicity. The copolymers less than 31 mol% of VA units were insoluble in water at any temperature. When the VA ratio increased to 45 mol%, the copolymer was soluble in water at room temperature, and the solution became turbid upon heating (Fig. 5B): it exhibited a lower critical solution temperature (LCST)-type thermal response. The thermo-responsive behavior was further investigated through variable-temperature transmittance measurement of the solution at 2 mg mL<sup>-1</sup> (Fig. 5C and S37, heating rate: 1 °C min<sup>-1</sup>;  $\lambda = 670$  nm). The transmittance gradually decreased to 10% around 40–70 °C and the cloud point ( $T_{\text{CP}, 50\%}$ : the temperature giving 50% transmittance) was determined to be 49.3 °C. The thermal response was also confirmed by temperature-variable dynamic light scattering (DLS) analysis: the hydrodynamic diameter ( $D_h$ ) gradually increased from ~50 nm to ~430 nm upon heating (Fig. S38). The copolymer is soluble in water due to

**A**

| VA/IPA | water  | MeOH  | EtOH  | DMF   | chloroform | acetone |
|--------|--------|-------|-------|-------|------------|---------|
| 100/0  | Sol    | Insol | Insol | Insol | Insol      | Insol   |
| 84/16  | Sol    | Sol   | Insol | Sol   | Insol      | Insol   |
| 73/27  | Sol    | Sol   | Sol   | Sol   | Insol      | Insol   |
| 57/43  | T-Res. | Sol   | Sol   | Sol   | Insol      | Insol   |
| 45/55  | T-Res. | Sol   | Sol   | Sol   | Insol      | T-Res.* |
| 31/69  | Insol  | Sol   | Sol   | Sol   | Sol*       | T-Res.* |
| 18/82  | Insol  | Sol   | Sol   | Sol   | Sol*       | T-Res.* |
| 7/93   | Insol  | Sol   | Sol   | Sol   | Sol        | T-Res.* |
| 0/100  | Insol  | Sol   | Sol   | Sol   | Sol        | Insol   |

2 mg/mL, Sol: soluble, Insol: insoluble, T-Res.: thermal response  
\*: There were a few undissolved portions.

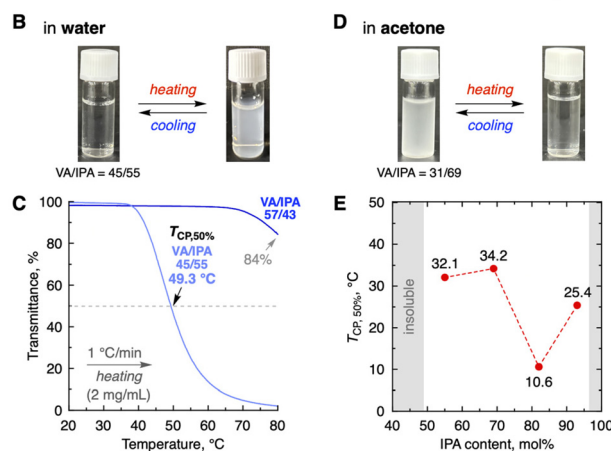


**Fig. 5** (A) Visual solubility test in water and several organic solvents for the resulting VA-IPA (co)polymers. (B) Photos showing the thermal response behavior of VA-IPA copolymers (VA/IPA = 45/55) in water (2 mg mL<sup>-1</sup>). (C) Temperature-variable transmittance measurement ( $\lambda = 670$  nm) on the heating process (1 °C min<sup>-1</sup>) with 2 mg mL<sup>-1</sup> solutions in water. (D) Photos showing the thermal response behavior of VA-IPA copolymers (VA/IPA = 31/69) in acetone (1.3 mg mL<sup>-1</sup>). (E)  $T_{\text{CP}, 50\%}$ -IPA content plot observed in the cooling process (1 °C min<sup>-1</sup>) with saturated (VA/IPA = 45/55: 0.9 mg mL<sup>-1</sup>, 31/69: 1.3 mg mL<sup>-1</sup>, 18/82: 1.7 mg mL<sup>-1</sup>, 7/93: 1.3 mg mL<sup>-1</sup>) solutions in acetone.

the hydration of VA-rich segments with water molecules at a lower temperature, and probably, dehydration from polymer chains occurs upon heating due to the entropic driving force. The chains aggregate through the hydrophobic interactions derived from IPA-rich segments giving the turbid solution. The copolymer of 57/43 also showed thermal response at a higher temperature (~80 °C) and the transmittance decreased only slightly.

Although PVA is known to be insoluble in most organic solvents, the VA-IPA copolymers became soluble in organic solvents such as methanol, ethanol, DMF and chloroform (Fig. 5A). The loss of crystallinity observed in the copolymers suggests that the chain-chain interactions through hydrogen bonding among hydroxyl groups are weakened, which likely accounts for their enhanced solubility compared with PVA. Interestingly, the IPA-rich copolymer (IPA content: 55 mol%–93 mol%) exhibited a distinctive upper critical solution temperature (UCST)-type thermal response in acetone; it was soluble at higher temperature and became insoluble upon



cooling (Fig. 5D). Both PVA and PIPA homopolymers were insoluble in acetone at any temperature due to their well-packed crystalline structures, indicating that the solubility or UCST behavior of the copolymer is truly unique. Variable-temperature transmittance measurements revealed that the cloud point ( $T_{CP,50\%}$ ) in the UCST behavior did not change monotonically with the unit ratio of the copolymer. Notably, the 18/82 copolymer gave the lowest  $T_{CP,50\%}$  among the four copolymers, indicating that it exhibits the highest solubility in acetone within a series (Fig. 5E and S39). The complicated solubility trend is likely governed by a delicate balance between the interactions among polymer chains and interactions with solvent molecules. The solubility uniqueness is reminiscent of the higher solubility of methylated cellulose in water compared with unmodified cellulose and is particularly intriguing as a characteristic unique to hydroxyl-containing polymers.<sup>29</sup> DLS analysis of the 45/55 copolymer (0.9 mg mL<sup>-1</sup> in acetone) exhibited the formation of huger aggregates than those in aqueous solution:  $D_h$  gradually increased from ~200 nm to ~2.4  $\mu$ m in the cooling process from 50 °C to 10 °C (Fig. S40). Thus, the controlled introduction of  $\alpha$ -methyl groups into PVA was found to be helpful for modulating the solubility and thermal response not only in water but also in organic solvents.

## Conclusion

In conclusion, we established an efficient synthetic route to vinyl alcohol (VA)-isopropenyl alcohol (IPA) copolymers using two types of alkenylboron monomers. Radical copolymerization of vinyl-type VBaam-MOE with isopropenyl-type IPBpin and side-chain oxidation afforded a series of VA-IPA statistical copolymers with various composition ratios (VA/IPA = 84/16–7/93), which were difficult to synthesize from acetyl-type precursors (*i.e.*, VAc and IPAc). The resulting copolymers were found to be amorphous at most composition ratios, whereas both VA and IPA homopolymers exhibited distinctive semi-crystalline nature. The introduced  $\alpha$ -methyl groups dramatically enhanced solubility in organic solvents such as methanol and DMF. The thermal response in the solution state depended on the composition ratio; copolymers with 43–55 mol% IPA units showed LCST-type thermos-responsive behavior in water and those with 55–93 mol% IPA units gave UCST-type response in acetone. Since PVA has been widely used for many applications as described above, the unprecedented syntheses of  $\alpha$ -methylated PVAs for allowing the modulation of physical properties is useful for accessing PVA-based materials with innovative functions in the future.

## Conflicts of interest

The authors declare no competing financial interests.

## Data availability

The data supporting this study have been included as part of the supplementary information (SI). Supplementary information: detailed description of synthetic procedures, experimental methods, <sup>1</sup>H NMR and FT-IR spectra, GPC analysis, DSC measurements, XRD measurements, UV-vis measurements and DLS measurements. See DOI: <https://doi.org/10.1039/d5py01168j>.

## Acknowledgements

The authors thank Prof. Takaya Terashima (Kyoto University) for fruitful discussions. This work was supported by JSPS [KAKENHI grants 23KJ1374 (H. S.), 22K14724 (T. N.), 25H02028 in Transformative Research Area (A) 24A202 (T. N.), and 24H00052 (M. O.)], JST [Grant No. JPMJPR23N6 (PRESTO, T. N.) and JPMJCR23L1 (CREST, M. O.)].

## References

- H.-K. Park, B.-S. Kong and E.-S. Oh, *Electrochem. Commun.*, 2011, **13**, 1051–1053.
- L. Liu, M. Wei, H. Li, Y. Chen, Y. Jiang, T. Ju, Z. Lu, G. Mu, L. Cai, D. Min, Y. Xie, J. Li and S. Xiao, *Green Chem.*, 2024, **26**, 11873–11884.
- M. Aslam, M. A. Kalyar and Z. A. Raza, *Polym. Eng. Sci.*, 2018, **58**, 2119–2132.
- Y. Li, J. Xie, H. Cheng, X. Wei, J. Chen, L. You and W. Chen, *Soft Matter*, 2025, **21**, 3148–3167.
- I. Sakurada, *Polyvinyl Alcohol Fibers*, Marcel Dekker, New York and Basel, 1985.
- S. Matuzawa and K. Ogasawara, *Angew. Makromol. Chem.*, 1972, **23**, 157–167.
- P. Chetri and N. N. Dass, *Polymer*, 1997, **38**, 3951–3956.
- H. Ochiai, H. Fujii, M. Watanabe and H. Yamamura, *Polym. J.*, 1974, **6**, 396–402.
- B. Y. Zaslavsky, L. M. Miheeva, S. V. Rogazhin, Y. A. Davidovich, A. V. Gedrovich, A. V. Shishkov, A. A. Gasanov and A. A. Masimov, *J. Chromatogr. A*, 1984, **291**, 203–210.
- M. Takahashi, K. Tashiro and S. Amiya, *Macromolecules*, 1999, **32**, 5860–5871.
- J. Lange and Y. Wyser, *Packag. Technol. Sci.*, 2003, **16**, 149–158.
- C. Maes, W. Luyten, G. Herremans, R. Peeters, R. Carleer and M. Buntinx, *Polym. Rev.*, 2018, **58**, 209–246.
- L. Jiang, T. Yang, L. Peng and Y. Dan, *RSC Adv.*, 2015, **5**, 86598–86605.
- N. G. Gaylord and F. R. Eirich, *J. Polym. Sci.*, 1950, **5**, 743–744.
- N. G. Gaylord and F. R. Eirich, *J. Am. Chem. Soc.*, 1952, **74**, 337–342.



- 16 Y. Kuwae, M. Kamachi and S. Nozakura, *Macromolecules*, 1986, **19**, 2912–2915.
- 17 T. Nishino, N. Kitamura and K. Murotani, *J. Polym. Sci., Part A: Polym. Chem.*, 2009, **47**, 754–761.
- 18 G. Takahashi and I. Sakurada, *Kobunshi Kagaku*, 1956, **13**, 497–502.
- 19 M. Ibonai, *Polymer*, 1964, **5**, 317–319.
- 20 T. Nishikawa and M. Ouchi, *Angew. Chem., Int. Ed.*, 2019, **58**, 12435–12439.
- 21 T. Nishikawa and M. Ouchi, *Chem. Lett.*, 2021, **50**, 411–417.
- 22 T. Nishikawa, *Polym. J.*, 2024, **56**, 873–886.
- 23 T. Nishikawa, *Bull. Chem. Soc. Jpn.*, 2025, **98**, uoae129.
- 24 T. Kanazawa, T. Nishikawa and M. Ouchi, *Macromolecules*, 2024, **57**, 6750–6758.
- 25 H. Suzuki, T. Nishikawa and M. Ouchi, *J. Am. Chem. Soc.*, 2025, **147**, 12672–12685.
- 26 In the synthesis of PVA homopolymers by boron-pendant oxidation, the resulting polymers spontaneously precipitate during the reaction. Then, most of the byproducts can be removed by simple filtration, and the residual byproducts are removed by the following dialysis. However, in the case of VA–IPA copolymers, the purification through reprecipitation and filtration does not work due to their high solubility in organic solvents, making the removal of anthranilamide-derived byproducts more difficult.
- 27 H. E. Assender and A. H. Windle, *Polymer*, 1998, **39**, 4295–4302.
- 28 We have synthesized PIPA from IPBpin in our previous study. At that time, DSC was performed below 80 °C and the crystalline properties were not fully characterized.
- 29 M. L. Coughlin, L. Liberman, S. P. Ertem, J. Edmund, F. S. Bates and T. P. Lodge, *Prog. Polym. Sci.*, 2021, **112**, 101324.

